Technical Report for DE-FG02-03ER46029
Sugar-Coated PPEs, Novel Nanomaterials and Sensing Modules for Disease and Bioterrorism Related Threats

PI Uwe Bunz; Email uwe.bunz@chemistry.gatech.edu

1) Introduction:

The detection and sensing of biological warfare agents (Ricin, Anthrax toxin), of disease agents (cholera, botulinum and tetanus toxins, influenza virus etc) and of biologically active species is important for national security and disease control. A premiere goal would be the simple colorimetric or fluorimetric detection of such toxins by a dipstick test. It would be desirable to sense 5,000-10,000 toxin molecules, i.e. 10-100 fg of a toxin contained 1-5 mL of sample. Fluorescent conjugated polymers should be particularly interesting in this regard, because they can carry multiple identical and/or different recognition units. Such an approach is particularly valuable for the detection of lectin toxins, because these bind to oligomeric carbohydrate displays. Lectins bind multivalently to sugars, i.e. several covalently connected sugar moieties have to be exposed to the lectin at the same time to obtain binding. The requirement of multivalency of the lectin-sugar interactions should allow a very sensitive detection of lectins with sugar coated conjugated polymers in an agglutination type assay, where the fluorescence of the PPEs disappears upon binding to the lectins. *High molecular weightsof the used PPEs would mean high sensitivity*. Herein we present our progress towards that goal up to date.

Table 1. Representative Examples of Sugar-Pathogen Interactions

Pathogen/Toxins	Disease	Sugar analyte
Influenza virus	respiratory disease, pneumonia	sialyl-oligosaccharides,
Coronavirus	common cold, pharyngitis	neuraminic acid-5,9-diacetate
HIV-1	AIDS	galactosyl ceramide
E. coli Enteroaggregative	food poisoning	Gal(α1,4)Gal on glycolipid
Heliobacter pylori	gastroduodenal ulcers	Lewis(b) blood group antigen
Staphylococcus	urinary tract infection	terminal GalNac
Enterococcus faecalis	diarrhea	extracellular galactose and fucose
Vibrio cholerae	cholera toxin	Gal-contianing oligosaccharide
Closteridium tetani	tetanus toxin	neuraminic acid derivatives
Closteridium botulinum	botulinum toxin	Gal(β)ceramide
Protein of Castor Bean	ricin toxin	galactose/N-acetylgalactosamine

Examples from: Mammen, M.; Choi, S.-K.; Whitesides, G. M. Angew. Chem. ***1998***, 37, *2754-2794."Polyvalent interactions in biological systems: Implications for design and use of multivalent ligands and inhibitors".*

To explore the field of water-soluble conjugated polymers as fluorecent sensors for toxins, fundamental questions have to be addressed: 1) *Synthesis* of water-soluble conjugated polymers of the PAE type. 2) Influence of the aqueous solvent upon the *fluorescence quantum yield* of the utilized conjugated polymers. This topic includes exploration of ways to increase/modulate fluorescence quantum yields of water soluble conjugated polymers by addition of surfactants or other additives, 3) *Attachment of sugar molecules* to the conjugated polymers, via long flexible chains. 4) *General sensing strategies* for biological moieties by water soluble conjugated polymers; 5) *Development of a viable analytical protocol* to sense lectins. This protocol has to include negative controls and sensing under realistic conditions.

We will discuss progress in fields that range from synthesis of water soluble, sugar coated PAEs to microstructuring of PAEs and to first model reactions for the sensing of proteins by a PPE model system.

2) A Model System for the Detection of Bioagents[6]

Efficient fluorescence and chromic behavior make poly(paraphenyleneethynylene)s (PPE) attractive as candidates in sensory schemes[1] and water soluble PPE-derivatives are known. However, PPEs substituted with biogenic moieties are largely uncharted waters,[10] and we were interested in a biotin-substituted PPE as model compound to study interactions of suitably functionalized conjugated polymers with bacterias. In this study, a streptavidin coated polystyrene bead is a primitive model polymer and "cell surface". To obtain a biotinylated PPE, the polymer **1** was dissolved in dry THF and treated with the biotin-attached acid chloride **2** at 0 °C. The acid chloride **2** was prepared according to literature procedures.[6] After allowing the reaction mixture to reach ambient temperature stirring was continued for 4h. The reaction mixture was precipitated into 250 mL methanol under vigorous stirring. The polymer **3** was isolated by suction filtration, re-dissolved in 1 mL of THF and precipitated into water to remove all excess of biotin. The successful biotinylation was qualitatively evidenced by IR spectroscopy of the polymer **3,** while its approximate degree of biotinylation was determined by an agglutination assay

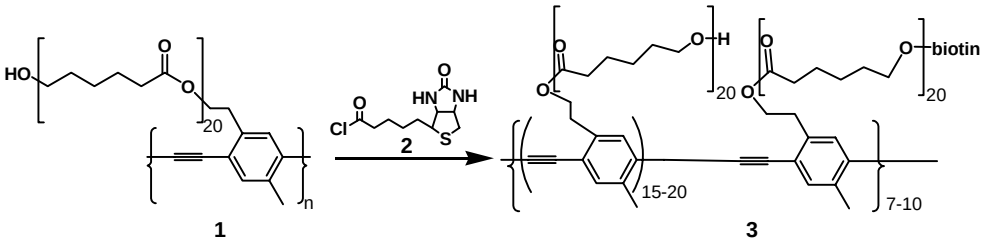

1 **3**

Scheme 1. Synthesis of a biotinylated PPE

utilizing free streptavidin.

Figure. 1. left: composite of **3** and streptavidin-coated microspheres agglutinated at the bottom of the Eppendorf cap. The blue fluorescence stems from the Eppendorf cap. Right: control experiment in which **2** and streptavidin coated microspheres are mixed. No agglutination is observed.

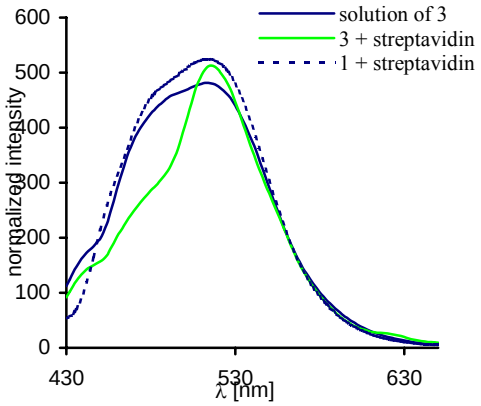

Figure. 2. Emission spectra of **3** (blue line), **1** with streptavidin (blue dotted line) and **3** with streptavidin (green line; suspension)

Based upon this assay every 10th to 20th monomer unit in the PPE chain (P_n = 140, gel permeation chromatography) was biotinylated. As a consequence only 7-14 biotin units are attached to a single polymer chain. This low "loading" of the PPE made it impossible to evidence the presence of biotin by ^{1}HNMR spectroscopy. However, the agglutination studies showed convincingly the presence of biotinylated PPEs. It was of interest to see if the biotinylated PPE **3** and its precursor **1** would behave differently when exposed to streptavidin-coated microspheres. In a first experiment polymer **1** was mixed with streptavidin-covered microspheres. Figure 1 (right) shows that the polymer solution is unchanged and does not alter its emission color. If a solution of **3** was mixed with a suspension of streptavidin-coated microspheres (Figure 1 left), the polymer precipitated out as a

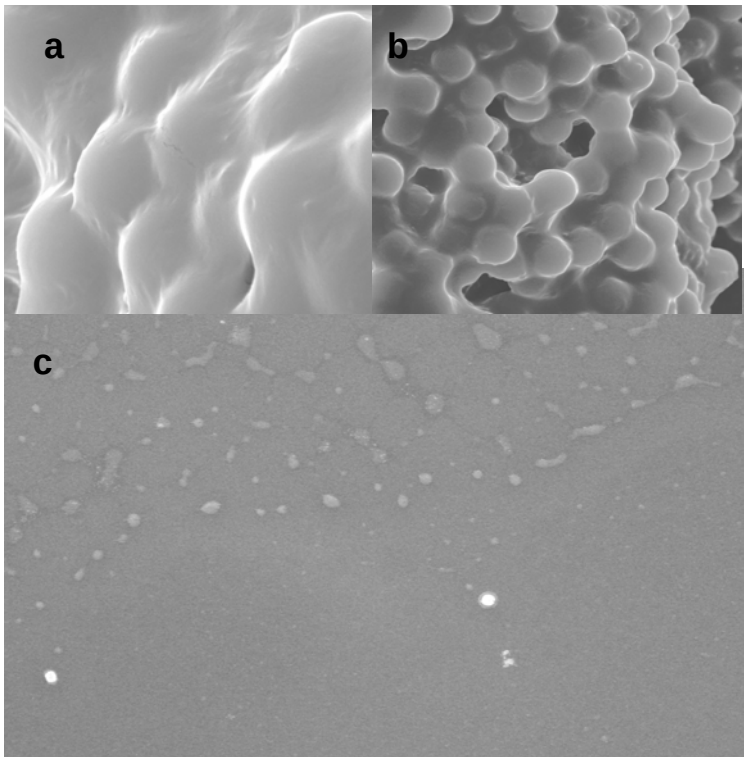

Figure 3. Scanning electron micrographs of a) complex of **3** and streptavidin-coated microspheres (18 μm x 18 μm), b) same as in a) but with lower magnification (53 μm x 53 μm), c) control experiment in which non-biotinylated polymer **1** is co-precipitated with streptavidin-coated microspheres. There is no apparent interaction between polymer (islands on top half) and microspheres (bottom white spots, size 452 μm x 452 μm.). The size of the microspheres is in all cases 5 μm.

consequence of the tight binding of the polymer bound biotin to the immobilized streptavidin. The precipitate obtained by the reaction of **3** with streptavidin-coated beads was examined by fluorescence microscopy.

The formation of dense "mats" of beads was observed. Surprisingly the beads appeared both blue and red fluorescent when viewed through a DAPI or Texas Red filter respective. Preparations of polymer **1** exposed to streptavidin beads produced isolated islands of fluorescence upon co-evaporation under otherwise identical conditions. The isolated islands of fluorescence are only visible under a DAPI filter, while under a Texas Red filter the sample is non fluorescent. To explain this behavior we took emission spectra of **3** in solution, **1** with streptavidin in solution and the complex of **3** with streptavidin as a suspension. The change in fluorescence is significant (Figure 2) and the aggregation causes a disappearance of the blue shoulder visible for (**1** + streptavidin) and for uncomplexed **3**.

To get a better idea of the microstructure of this composite, we performed scanning electron microscopy of the complex. In Figure 3a. the egg crate structure of the composite is visible. The conjugated polymer covers the beads evenly giving testimony to the binding between biotin and streptavidin. In Figure 3b. the three dimensional arrangement of the polymer covered beads is apparent. The control experiment (**1** + streptavidin-coated beads) on the other hand (Figure 3c) does not show *any* defined structure, only islands of polymer **1** are visible in the upper half, while three streptavidin-coated beads are isolated in the lower half of the picture.

In conclusion we have demonstrated that lightly biotin functionalized PPEs form nanocomposites with streptavidin coated microspheres. This primitive system can be seen as a model for the interaction of cells (emulated by the beads) with functionalized conjugated polymers that could play an important role in the simple, colorimetric of fluorimetric detection of pathogens and toxins by PPE-types. The lowest amount of streptavidin we are able to detect now is in the single-digit ng range.

3) Synthesis of novel polymer backbones and monomers

An important subgoal of this project was to obtain PPE derivatives that could easily be post-functionalized. An azide group in the side chain of the PPEs should be ideal. The azide functionality is quite robust and survives the conditions of the Pd-catalyzed coupling to afford a PPE in which every second unit displays an azide functionalized side chain (Scheme 2). Azides are versatile, because they can partake in 1,3-dipolar cycloadditions to "click on" biologically active or solublilizing agents. The 1,3-dipolar cycloadditions have been investigated in depth by Huisgen,[9] and utilizied recently by Sharpless.[9] We think that this cycloaddition approach will have great potential for postfunctionalization of **8**. The synthesis of the azide monomer **7** starts with the conversion of the hydroxy group of **4** into an iodide (**6**). Reaction with sodium azide then furnishes **7**. The azide group survives the Pd-catalyzed coupling of the Heck-Sonogashira type without any problem. Side products due to competing 1,3-dipolar cycloadditions are not observed at 30-50°C. At the moment we perform model reactions with the azide monomer **7** to determine how to best attach biological molecules of interest (sugars, small peptides). At the same time we have discovered that heating thin films of polymer **8** under nitrogen to 300°C gives a fluorescent yet crosslinked and insoluble conjugated polymer film.

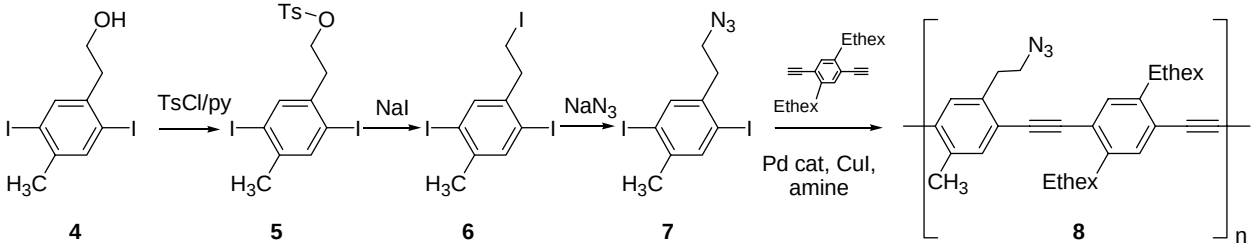

Scheme 2. Synthesis of an azide-substituted PPE.

Synthesis of monomers. To increase water solubility a triethyleneglycol monomer **11** was made by reacting diiodohydroquinone with 8-iodo-2,5-dioxaoctanol in boiling acetone in the presence of potassium carbonate. We are investigating the synthesis of PPE type polymers from **11** and their use as water soluble and processible PPEs. In the next step we can either attach propargylic groups to the side chains or we can convert them into azide functionalities for further manipulation. Azide substituted PPEs will be valuable because the propargylated sugar **12** (has already been synthesized) will be "clicked on" by a 1,3-dipolar cycloaddition.[9]

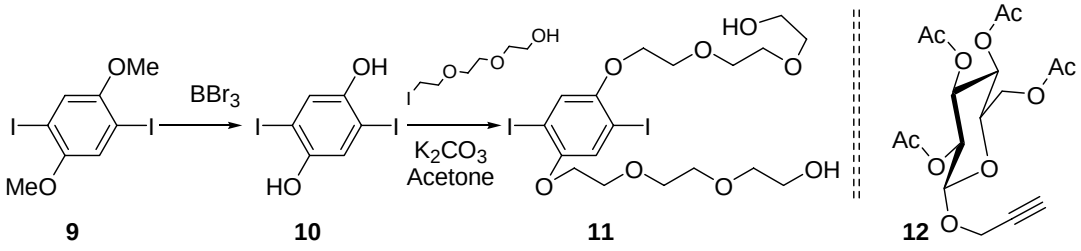

Scheme 3. Synthesis of a oligoethyleneglycol substitutet monomer for the synthesis of water soluble poly(*para*phenyleneethynylene)s.

4) "Surfactochromic" Conjugated Polymers: Surfactant Effects on Sugar-Substituted PPEs

Whitten demonstrated that the interaction of a negatively charged, water soluble conjugated polymer of the poly(*para*-phenylenevinylene) PPV type with cationic surfactants (in water) leads to a dramatic increase of the fluorescent quantum yield of the PPV, however, without a large change of the emission wavelength.[1,2] Water quenches the fluorescence of conjugated polymers. The large relative increase of the quantum yield of the PPV upon addition of the surfactant "restores" the fluorescence intensity to that observed for similar PPVs in organic solvents. It is proposed to call the change of optical properties of conjugated materials upon addition of surfactants "surfactochromicity". This effect must be of great importance in the application of conjugated polymers for biosensory processes where issues of signal enhancement and suppression play a crucial role.[3-6]

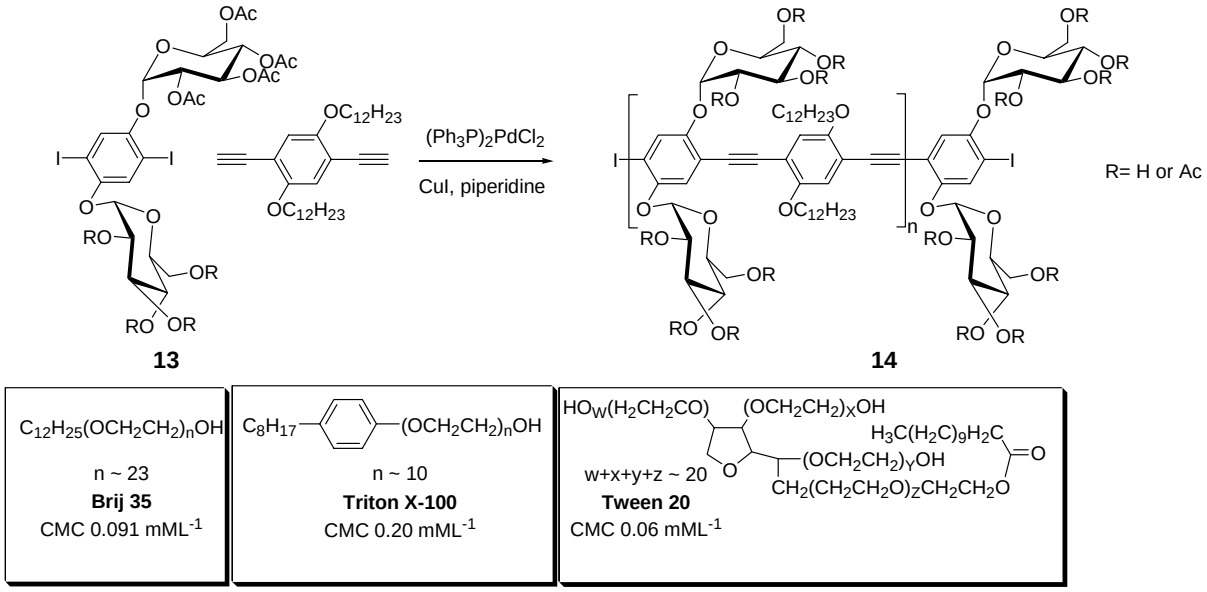

Scheme 4. Utilized PPE-type polymer **14** and surfactants including critical micelle forming concentrations (CMC).

While the interaction of conjugated polyelectrolytes with oppositely charged surfactants or amphiphilic counter ions is strong and well-established,[1-4] the interaction of non ionic water soluble conjugated polymers with non-ionic surfactants has not been studied. Such systems should likewise be surfactochromic and will have great potential in biosensory and biodevice applications.[6,7]

The water soluble sugar-substituted PPE **14** undergoes surfactochromic changes in emission[8,10] in the presence of the non-ionic amphiphiles Brij 35, Triton X-100, and Tween 20.[11] The absorbance of **14** shows little to no change upon varying surfactant type (Tween 20, Triton X-100, Brij 35, cetyltrimethyl-ammonium bromide (CTAB), cetylpyridinium chloride (CPC) and sodium dodecyl sulfate (SDS)) or concentration (1% to 10% surfactant). The Uv-vis spectrum of **14** in water/buffer/detergent mixtures is identical to the absorbance of dialkoxy-PPEs in chloroform,[12] suggesting that the backbone of **14** is non-planarized under these conditions.

The polymer **14** was obtained by a Pd-catalyzed coupling[10] of the bis-glucosylated diiodide **13** with 1,4-diethynyl-2,5-bisdodecoxybenzene under standard conditions.[13] Approximately half of the acetyl groups fall off during the coupling, with piperidine acting as a deacetylation reagent, so that R = either H or Ac.

The loss of acetyl groups was quantified by ^{1}H NMR and by IR spectroscopies.[14] The resulting polymer is soluble in water, DMSO, and in THF.

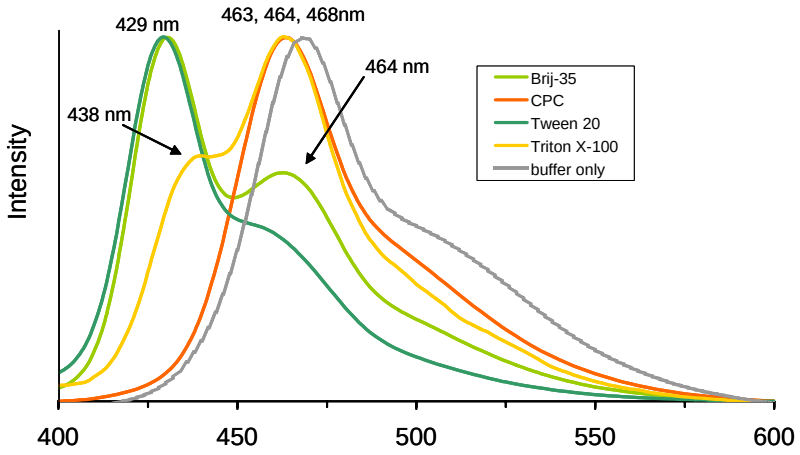

Figure 4. Emission spectra of **14** in different surfactants (0.5 mgL^{-1} polymer in phosphate buffered saline (PBS), 10% w/v surfactant, λ_{ex} 385 nm, 25^{o}C): (—) PBS, no surfactant; (—) cetylpyridinium chloride (CPC); (—) Triton X-100 (160 mM); (—) Tween 20 (81 mM); (—) Brij 35 (82 mM). The emission spectra were normalized so that the emission maxima of all the samples are identical.

In water **14** shows a relatively weak emission at 468 nm with a shoulder at 512 nm (Figure 4).[8-10] Addition of the ionic surfactants CTAB, CPC or SDS leads to a small blue shift in fluorescence and decreases the emission at 512 nm. The presence of nonionic surfactants provides a large response in the emission of **14**. The presence of Triton X-100 induces a subtle shift, the emission of **14** begins to display a shoulder around 430 nm, providing evidence that the polymer aggregates are being broken up. The presence of Brij 35 causes an increase in the 430 nm peak while diminishing the 460 nm emission of **14**. After the addition of Tween 20 the solution of **14** shows a small shoulder in the emission of **14** at 460 nm with the emission at 429 nm being most intensive. The apparent trend for disassembling aggregates of **14** suggests that the deaggregating power of the surfactants is Tween 20 > Brij 35 > Triton X-100 and stems probably from the enhanced solubilization of the sugar side chains in **14** by Tween. Importantly, these effects are only evident in emission and not in absorption suggesting that the planarization of the backbones of the PPEs does not play a large role under these conditions (Figure 4).

Besides surfactant type, it was of interest how surfactant concentration would affect the optical properties of **14**. In Figures 5 and 6, the data is normalized to best display the changes in the *shape* of the emission spectra. In Figure 5a the shape of the curve changes, exhibiting a subtle blue-shift, as surfactant concentration is increased suggesting dissolution of polymer aggregates. Upon addition of Triton X-100 the emission intensity of **14** increases 20-fold. This behavior is similar to Whitten's observation of increased fluorescence of PPVs upon addition of ionic surfactants.[1]

Figure 5b shows a marked change in the spectral shape of **14** upon the addition of Tween 20. As suggested by the data in Figure 4, Tween 20 is an excellent solvating agent for **14**. A complete disappearance of the aggregate band at 520 nm is observed as surfactant is added. A nearly complete conversion to the low wavelength band at 430 nm suggests almost full de-aggregation. Finally, it is interesting to note the dramatic change of emission wavelength upon addition of higher concentrations of Brij 35 to **14**. Low concentrations of Brij, up to 8 mM (1%), have virtually no effect on the aggregation of **14**, however, at higher concentrations, near complete breakup of the aggregates of **14** is recorded. This

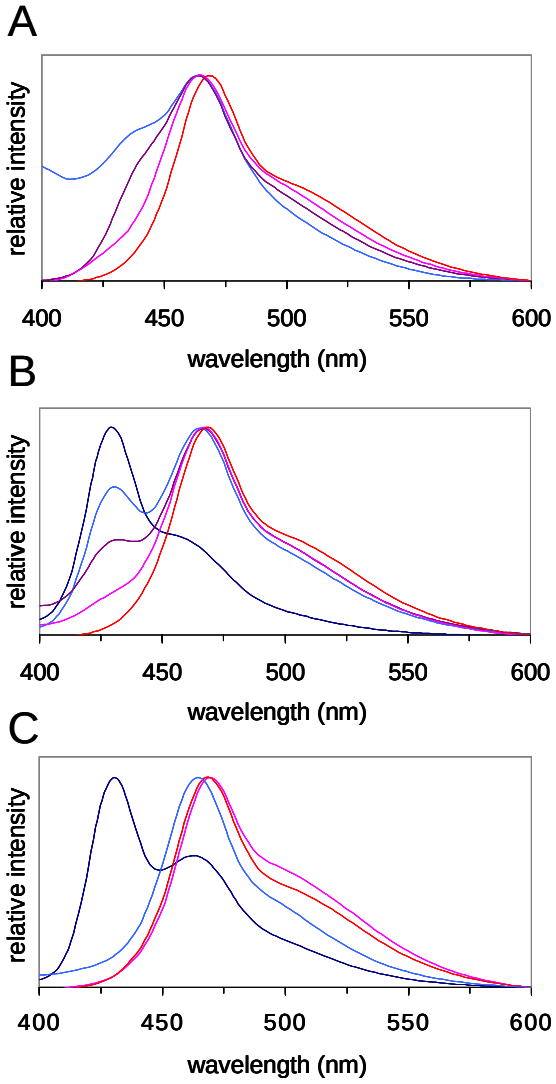

case is similar to the one where Tween 20 was added to **14** suggesting a critical surfactant de-aggregation concentration. These effects are only observed in a regimen that is significantly above the critical micelle forming concentration (CMC) of the surfactants under observation (see Scheme 1 for the CMC of Triton X-100, Brij 35 and Tween 20).[11]

The temperature dependence of the emission of **14** in the presence of surfactants was examined. It would be expected that an increase in temperature would enhance solubility of **14** either with or without surfactant present. Additionally, one would expect to see blue-shifted emissions resulting from this improved dissolution of aggregates (Figure 6). In the presence of Brij 35, an increase in the emission intensity of **14** was observed with no blue-shift and with Triton X-100 added an increase in emission intensity of **14** was accompanied by the expected blue-shift of the emission. In the absence of surfactant a *decrease* in the intensity of the emission from **14** was observed with a relative increase in the aggregation band of **14** centered at 520 nm. Similarly, with Tween 20 as the surfactant, a rise in temperature resulted in a decrease in emission intensity of **14** as well as a red-shift. Several conclusions can be gleaned form this data: 1) Nonionic surfactants interact with **14** in an aqueous environment at surfactant concentrations that are well above the CMC leading to a blue shifted emission and a break-up of aggregates of **14** (Tween 20, Brij 35) or to 20-fold enhanced emission (Triton X-100). The blue shift

Figure 5. Normalized emission spectra of **14** in different surfactants varying their concentrations (0.5 mgL^{-1} **14** in phosphate buffered saline plus surfactant, λ_{ex} 385 nm, 25°C). A) Triton X-100: (—) PBS, 0%w/v surfactant, (—) 0.1%w/v surfactant (1.6 mM), (—) 1% w/v surfactant (16 mM), (—) 10% w/v surfactant (160 mM). B) Tween 20: (—) PBS, 0% surfactant, (—) 0.1%w/v surfactant (0.81 mM), (—) 0.5% w/v surfactant (4.1 mM), (—) 1% w/v surfactant (8.1 mM), (—) 10% w/v surfactant (81 mM). C) Brij 35: (—) PBS, 0% surfactant, (—) 1%w/v surfactant (8.2 mM), (—) 5% w/v surfactant (41 mM), (—) 10% w/v (82 mM) surfactant. The emission spectra were normalized so that the emission maxima of all the samples are identical.

is more pronounced the more concentrated the surfactant solution is. 2) Increase in temperature leads to enhanced emission of **14** for Brij 35 and for Triton X-100, while the emission intensity decreases for **14** in buffer (PBS) and interestingly as well in the presence of Tween 20.[15]

The emissive properties of a water soluble polymer such as **14** therefore can be easily manipulated by addition of nonionic surfactants. The fluorescence enhancement in particular will be critically important when exploring the lower threshold for the sensing of biological targets utilizing water soluble PPEs.

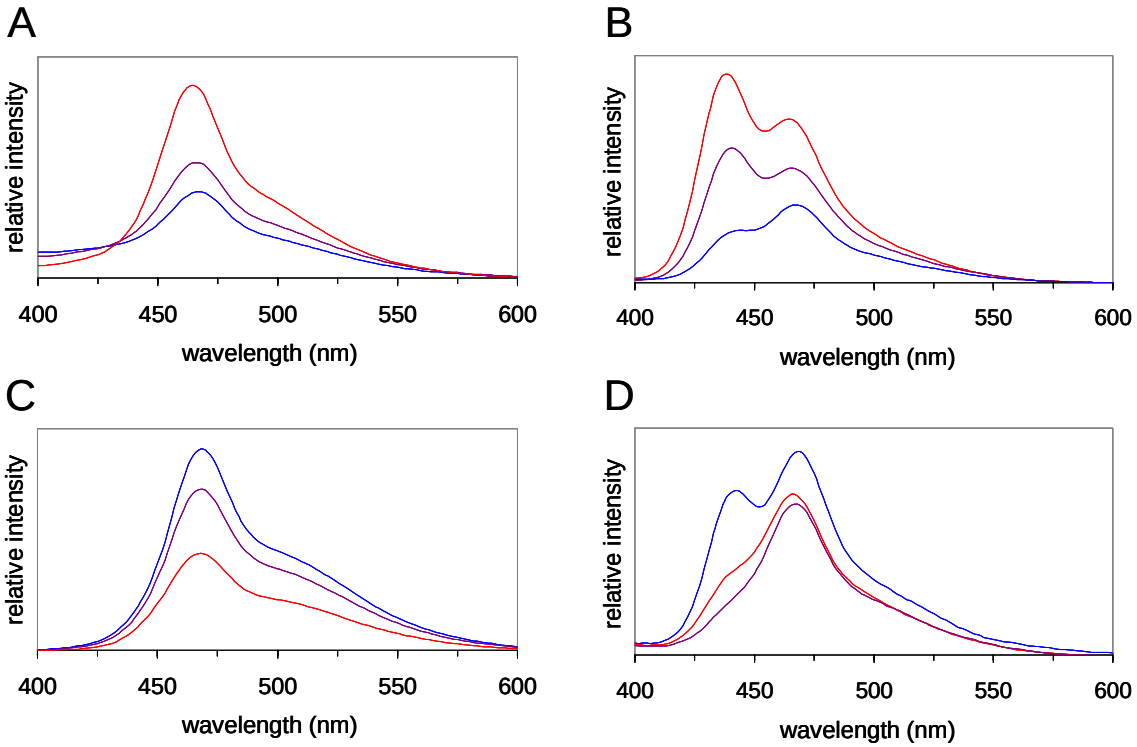

Figure 6. Emission spectra of **14** in different surfactants varying the temperature (0.5 mgL^{-1} **14** in phosphate buffered saline plus 5% surfactant, λ_{ex} 385 nm). A) Brij 35: (—) 25°C, (—) 50°C, (—) 75°C (41 mM). B) Triton X-100: (—) 25°C, (—) 37°C, (—) 50°C (80 mM). C) PBS, no surfactant: (—) 25°C, (—) 50°C, (—) 75°C. D) Tween 20: (—) 25°C, (—) 37°C, (—) 50°C (41 mM).

5) Novel Micro and Nanostructures from PPEs

We report the facile nanostructuring of conjugated polymers **15-19** into hexagonally ordered 2D arrays by evaporative cooling with the subsequent condensation of water droplets onto a dilute solution of polymer in carbon disulfide. This report is the first example in which rigid rodlike polymers are microstructured into inverse hexagonal arrays by the formation, and subsequent crystallization of "breath figures".[16,17]

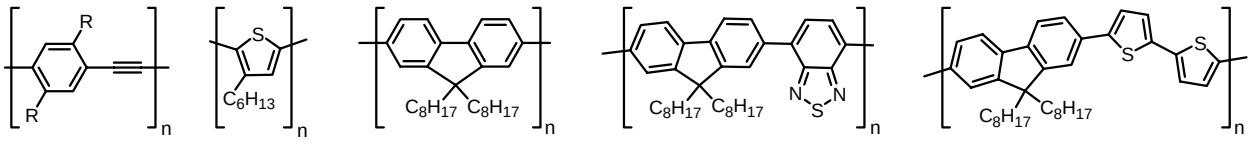

15 **16** **17** **18** **19**

Chart 1. Polymers for bubble formation. Substitution pattern for **15: a**, R = 2-ethylhexyl; **b**, R = hexoxy; **c**, R = -CH_2CH_2-O-Si(isopropyl)$_3$.

Micro- and nanostructuring[18-20] of fluorescent conjugated polymers is very important for potential biological applications. By pre-selecting the size of the micro or nanostructures the material would probably interact best with a specific biological species that fits well into the formed nanostructures. Micrometer sized structures would interact best with cells or bacteria, while structures in the nm scale would only allow the interaction with proteins of that specific size. Issues are the formation of such nanostructures and then the functionalization of their surfaces. In the short time since March of 2003 we

have been able to obtain a series of interesting nanostructures in collaboration with Prof. Mohan Srinivasaro (School of Polymer, Textile, and Fiber Engineering at Gatech), but we have not yet started to look into the manipulation of the side walls with biologically relevant species.

A variety of templating methods based on self-assembly have been used to create structures with micron and submicron dimensions. These include templating using ordered arrays of colloidal particles,[21-25] templating using an emulsion,[26] honeycomb structures formed by polymers with rod-coil architecture,[19,27-29] self-organized surfactants that generate mesoporous silica,[30-32] microphase separated block copolymers,[34,35] and even bacteria.[36] These templating approaches allow the preparation of macroporous materials that have three-dimensionally (3-D) ordered pores with dimensions of tens to thousands of nanometers.

Specifically, the mesostructuring of organic semiconductors and organic polymers often requires elaborate methods such as microemulsion processing, template-assisted self-assembly, aggregation of large graphitic hydrocarbon disks,[37] and lengthy crystallization methods. With exemption of the Neher-Scherf-Landfester microemulsion method[18] that had originally been developed by Stover[38] for non-conjugated polymers, and the recent nanotemplating approaches developed by Martin[39] and used by us,[40] there are not many generally applicable methods for the mesostructuring of rigid rods on the large nanometer and small micrometer scale. This is in stark contrast to the case of block copolymers, where a host of mesostructured systems is easily available by spontaneous self-assembly in the solid state. Particularly spectacular examples include Jenekhe's hollow spheres[19] and Wiesner's "Plumber's Nightmare".[41]

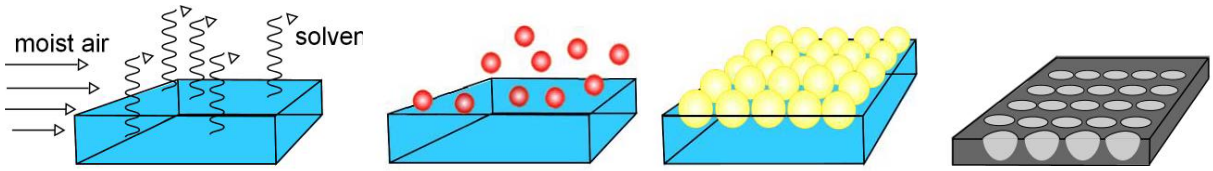

Figure 7. Mechanism of bubble array formation utilizing the breath figure method. a) moist air leads to evaporative cooling of the solvent carbon disulfide. b) Water droplets form by condensation of the warm moist air onto the cold surface of the liquid. c) The water droplets organize into a two dimensional hexagonal array. d) The water droplets sink into the solution and further evaporation leaves the polymer matrix that has formed by the imprinting of the bubbles as a fossil.

We demonstrate a simple procedure to create microstructured films of rodlike, conjugated polymers. The experiment consists of taking a dilute solution of a rodlike polymer (**15-19**, Chart 1; concentration approx. 1% by weight) and evaporating the solvent in a stream of moist airflow across the polymer solution surface. Structures shown in Figures 8-9 are gestate in a matter of a few seconds. This has been attributed to the formation of breath figures and their subsequent crystallization to develop the ordered array of holes on the polymer film (Figure 7).[16,17] When moist air is in contact with a cold surface (solid or a liquid), moisture condenses, forming water droplets that grow with time and form ordered patterns on the surface. Such a pattern formation has been termed "breath figures". The phenomenon of breath figures has been studied for over a century now starting with the early works of Lord Rayleigh,[17] Baker,[42] and Aitken,[43] and more recently by Knobler and Beysens.[44] Breath figures form on solids and as well on hydrophobic liquids, but are only of temporary nature. Should the same experiment be performed upon a solution of carboxylate terminated polystyrene in carbon disulfide (bp 46 ^{o}C), then the solvent evaporates and leaves the polymer shells as a nanostructured, highly ordered foam. This method has been used for the nanostructuring of star polystyrene and for rod-coil block copolymers that contain rigid segments such as poly(*para*phenylene)s or poly(*para*phenylenevinylene)s.

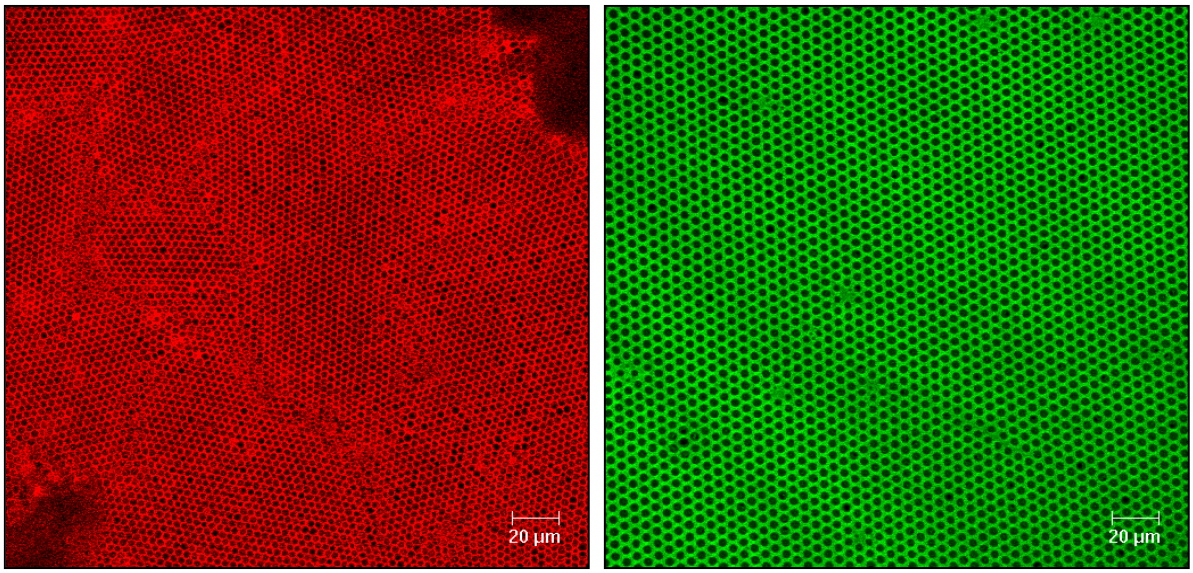

Figure 8. Hexagonal bubble arrays formed by evaporation of dilute solutions of conjugated polymers in carbon disulfide. Left: Bubble arrays formed from polythiophene **16**. Right, arrays formed from bisethylhexyl-PPE **15a**. The individual bubbles formed by **15a** and **16** are of similar size, but the domain size in **15a** is macroscopic and exceeds 1 mm x 1 mm, while the domain size in polythiophene **16** is 0.05 x 0.3 mm.

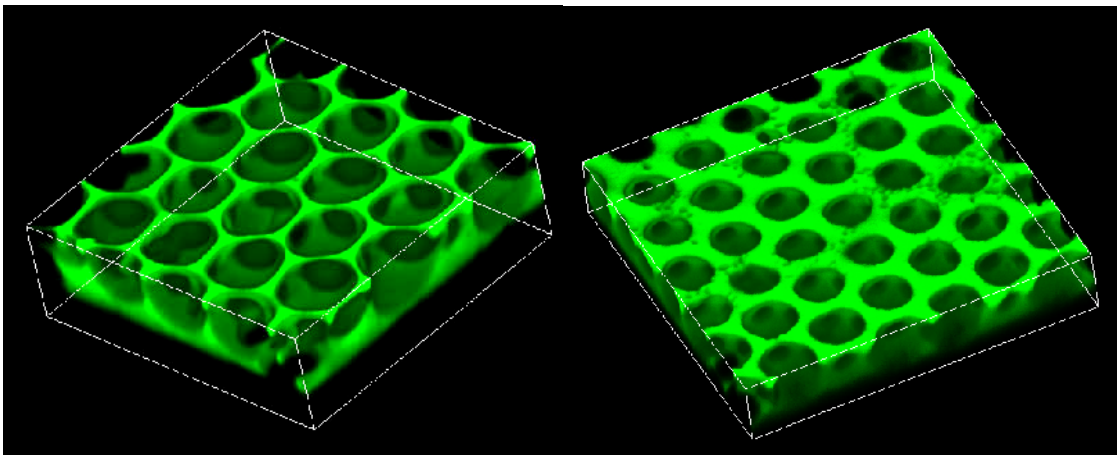

Figure 9. Confocal laser micrographs of monolayers of conjugated polymer matrices containing bubble arrays. Left: Bubbles formed from **15c**. Right: Bubbles formed from **15b**. The bubble arrays formed from **15c** are considerably more durable than those formed from **15b**. The bubble arrays formed from **15b** have thicker walls but are mechanically less stable than the arrays formed from either **15a** or **15b**. The bubbles are 3-5 µm large depending upon the specific conditions of preparation. Box size is 18 x 18 x 6.2 µm.

While a variety of polymers have been used with various architectures, they all have a polystyrene backbone or appendage as structurally unifying feature.[45] It is generally believed that polymers devoid of polystyrene in the backbone and rod-like polymers are not capable of forming these highly ordered inverted lattices. We were interested to refute this hypothesis, and hence used polymers **15-19** as substrates for bubble array formation**.**

Poly(*para*phenyleneethynylene) PPE **15a** was dissolved in carbon disulfide and a drop of this solution was placed on an untreated glass slide. Evaporation of the solvent in the presence of a moist airflow leads to the formation of ordered structures shown in Figures 8-9. Highly ordered arrays of holes with hexagonal symmetry are formed, with the order extending over a large area (over 1 mm^2) with almost no grain boundaries. If the experiment was repeated in the absence of moisture in the atmosphere, then one was left with a solid polymer film, devoid of ordered structure. This observation argues for the structure formation being due to "breath figures" and their subsequent crystallization.[16,17,42-45] Our model for the formation of the ordered macroporous structures is schematically illustrated in Figure 7.[16]

Due to the high vapor pressure of the solvent and the velocity of air across the surface, the solvent evaporates leading to rapid cooling of the surface. Temperatures near 0°C were measured in our experiments. This cooling leads to the nucleation and growth of water droplets that grow as a function of time.[16,36,42,44] The velocity of air, coupled with convection currents on the solution surface that are due to evaporation, drive the ordering and packing of the water droplets. This ordering of holes in the films into hexagonal arrays is not surprising, as it is well known that spheres pack with hexagonal packing on a surface.

Because carbon disulfide is heavier than water, only one layer of the bubbles form. By proper choice of solvents it is possible to form three-dimensionally ordered structures.[16] A number of factors influence the dimensions of the bubbles,[16] however, the primary factor that determines the size of the bubbles is the velocity of airflow across the polymer solution surface. In most methods of self-assembly the size of the structures are built in by the choice of the template used. However, in the structure formation reported here, the size of the structure can be *dynamically tuned* by proper choice of the velocity of airflow across the surface. In Figure 8 nanopores formed from bisethylhexyl-PPE **15a**[46] and from poly(hexylthiophene) **16**[47] are shown. The bubbles are approximately 3-4 μm in diameter and the microstructuring of **15a** occurs over a large macroscopic area, while **16** shows considerably smaller domains of highly ordered bubbles.

In Figure 9 confocal micrographs of two different PPEs **15b**[48] and **15c**[49] are shown. While both images look similar there is an interesting difference: PPE **1c** forms perfect and durable microstructures, while the dialkoxy-substituted PPE **15b** is mechanically and photochemically much less stable. PPE **15b** forms structures that are not as perfect, mechanically less durable, and display thicker walls. Attempts to utilize a PPE with a more hydrophilic side chain such as reported by us recently,[50] failed. Undefined blobs of air formed under those conditions. The method however works well for polyfluorenes **17** and their heterocyclic copolymers **18** and **19**.[51] These polymers give bubble arrays of excellent quality. The degree of polymerization does not seem to be a critical parameter in the formation of the ordered arrays.

In summary, we have reported a simple procedure for microstructuring conjugated, rodlike polymers. The fact that linear rigid rod polymers form highly ordered arrays of holes under most trivial experimental conditions convincingly refutes the notion that either highly branched or coiled (i.e. polystyrene) structural segments are necessary to generate these arrays. In future we will show that such arrays are useful in directed energy and charge transfer.

6) Conclusions and further directions

In conclusion we have made a series of new PPEs.

- These PPEs are water-soluble either because of the attachment of a macromolecular or a sugar substituent. It is possible to further functionalize the ends of the macromolecular substituents by biotin. The resulting biotinylated PPE is an excellent model sensor for streptavidin.

  It has been shown that the fluorescence quantum yield and the emission maximum of water soluble PPEs can be shifted by the addition of nonionic surfactants such as Brij 35 and Triton X-100: Those are additives that are regularly utilized by biologists.

- PPEs and other conjugated polymers are easily micro and nanostructured into novel bubble arrays. The size of these arrays can be varied by the experimental conditions. At the moment we attempt to make very small holes and we attempt to hydrophilize the holes to attach biologically active species such as sugars to the inner wall of these holes. Depending on the hole size different biological species should interact preferentially. If the holes are very small for example it is not expected that bacteria or cells will interact with the arrays, but proteins should. Larger holes should be better for the interaction with larger entities such as cells or microorganisms.

Publications that Acknowledge DOE funding

Y. Wang, B. Erdogan, J. N. Wilson, U. H. F. Bunz, Grafted conjugated polymers: synthesis and characterization of a polyester side chain substituted poly(para-phenyleneethynylene). *Chem. Commun.* **2003**, 1624-1625.

J. N. Wilson, Y. Wang, J. J. Lavigne, U. H. F. Bunz, A biosensing model system: selective interaction of biotinylated PPEs with streptavidin-coated polystyrene microspheres. *Chem. Commun.* **2003**, 1626-1627.

J. J. Lavigne, D. L. Broughton, J. N. Wilson, B. Erdogan, U. H. F. Bunz, Surfactochromic conjugated polymers: surfactant effect on sugar substituted PPEs. *Macromolecules* **2003**, *36*, in press.

L. Song, R. K. Bly, J. N. Wilson, S. Bakbak, J. O. Park, M. Srinivasarao, U H. F. Bunz, Facile Microstructuring of Organic Semiconducting Polymers by the Breath Figure Method: Hexagonally Ordered Bubble Arrays in Rigid Rod Polymers, *Adv. Mater. Submitted.*

References

1) (a) Chen, L. H.; Xu, S.; McBranch, D.; Whitten, D. *J. Am. Chem. Soc.* **2000**, *122*, 9302-9303. (b) Chen, L. H.; McBranch, D. W.; Wang, H. L.; Helgeson, R.; Wudl, F.; Whitten, D. G. *Proc. Nat. Acad. Sci.* **1999**, *96*, 12287-12292.

2) In a similar study Thünemann had demonstrated as early as 1999 that carboxylate-substituted PPEs can form complexes with cationic surfactants, but the utilized PPEs were not well-defined. Theextracted optical properties were difficult to interpret: (a) Thünemann, A. F. *Adv. Mater.* **1999**, *11*, 127-130. (b) Thünemann, A. F.; Ruppelt, D. *Langmuir* **2001**, *17*, 5098-5102 .

3) Ho, H. A.; Boissinot, M.; Bergeron, M. G.; Corbeil, G.; Dore, K.; Boudreau, D.; Leclerc, M. *Angew. Chem. Int. Ed. Engl.* **2002**, *41*, 1548-1551.

4) (a) Gaylord, B. S.; Heeger, A. J.; Bazan, G. C. *J. Am. Chem. Soc.* **2003**, *125*, 896-900. (b) Gaylord, B. S.; Wang, S. J.; Heeger, A. J.; Bazan, G. C. *J. Am. Chem. Soc.* **2001**, *123*, 6417-6418. (c) Fan, C. H.; Plaxco, K. W.; Heeger, A. J. *J. Am. Chem. Soc.* **2002**, *124*, 5642-5643.

5) (a) Ewbank, P. C.; Nuding, G.; Suenaga, H.; McCullough, R. D.; Shinkai, S. *Tetrahedron Lett.* **2001**, *42*, 155-157. (b) McCullough, R. D.; Ewbank, P. C.; Loewe R. S. *J. Am. Chem. Soc.* **1997**, *119*, 633-634.

6) Wilson, J. N.; Wang, Y. Q.; Lavigne, J. J.; Bunz, U. H. F. *Chem. Commun.* **2003**, 1626-1627.

7) Okada, S.; Peng, S.; Spevak, W.; Charych, D. *Acc. Chem. Res.* **1998**, *31*, 229-239.

8) (a) Halkyard, C. E.; Rampey, M. E.; Kloppenburg, L.; Studer-Martinez, S. L.; Bunz, U. H. F. *Macromolecules* **1998**, *31*, 8655-8659. (b) Miteva, T.; Palmer, L.; Kloppenburg, L.; Neher, D.; Bunz, U. H. F. *Macromolecules* **2000**, *33*, 652-654. (c) Kim, J.; Swager T. M. *Nature* **2001**, *411*, 1030-1034.

9) (a) Huisgen, R. *J. Org. Chem.* **1976**, *41*, 403-419. (b) Huisgen, R.; Szeimies, G.; Moebius, L. *Chem. Ber* **1967**, *100*, 2494-2499. (c) Huisgen, R.; Szeimies, G.; Moebius, L. *Chem. Ber* **1966**, *99*, 475. (d) Wang, Q.; Chan, T. R.; Hilgraf, R.; Fokin, V. V.; Sharpless, K. B.; Finn, M. G.; *J. Am. Chem. Soc.* **2003,** *125***,** 3192-3193. (e) Lee, L. V.; Mitchell, M. L.; Huang, S.-J.; Fokin, V. V.; Sharpless, K. B.; Wong, C.-H.; *J. Am. Chem. Soc.* **2003,** *125***,** 9588-9589. .

10) (a) Bunz, U. H. F. *Chem. Rev.* **2000**, *100*, 1605-1644. (b) Bunz, U. H. F. *Acc. Chem. Res.* **2001**, *34*, 998-1010. (c) Erdogan, B.; Wilson, J. N.; Bunz, U. H. F. *Macromolecules* **2002**, *35*, 7863-7864.

11) The CMC of the utilized non ionic surfactants can be found on www.sigmaaldrich.com in the technical section.

12) (a) Wilson J. N.; Bangcuyo, C. G.; Bunz, U. H. F. unpublished results; $\lambda_{max(absorption)}$ of both **14** as well as bisdodecoxy-PPE (in chloroform) are identical and appear at 450 nm (±5 nm).[10a] Upon planarization of dodecyloxy-PPE a red shift of $\lambda_{max(absorption)}$ to 478 nm is observed.

13) Experimental: The interactions between **14** and both ionic (cetyltrimethylammonium bromide (CTAB), cetylpyridinium chloride (CPC) and sodium dodecyl sulfate (SDS)) and nonionic surfactants (Brij 35, Triton X 100 and Tween 20) was examined. All studies were carried out in phosphate buffered saline (PBS; 50 mM phosphate pH 7.5, 150 mM NaCl, 2 mM KCl) with or without added surfactant. A PPE stock solution was made by dissolving **14** in DMSO **(**2 gL^{-1}). DMSO was utilized to insure complete solubility of **14** at the high concentration. The solubility of **14** does not exceed approx. 1mgL^{-1} in pure water. The stock solution of **14** was serially diluted with a surfactant stock solution prepared in water as necessary to provide solutions with varying surfactant concentrations and 0.5-5 mgL^{-1} PPE. Fluorescence emission spectra were recorded at 25, 37, 50 or 75^{o}C with excitation at 385 nm on a JASCO FP6200 fluorescence spectrometer equipped with a Peltier heating element. UV-vis spectra were taken on a JASCO V-500 spectrometer at ambient temperature.

14) Zhou, Q.; Swager, T. M. *J. Am. Chem. Soc.* **1995**, *117*, 12593-12602.

15) Kwak, J. C. T. (ed), Polymer-Surfactant Systems; *Surfactant Science Series* **1998**, *77*, whole issue.

16) Srinivasarao, M.; Collings, D.; Philips, A.; Patel, S. *Science* **2001**, *292*, 79.

17) Lord Raleigh, *Nature* **1911**, *86*, 416. Lord Raleigh, *Nature* **1912**, *90*, 436.

18) Kietzke, T.; Neher, D.; Landfester, K.; Montenegro, R.; Guntner, R.; Scherf. U. *Nature Mater.* **2003**, *2*, 406. Piok, T.; Gamerith, S.; Gadermaier, C.; Plank, H.; Wenzl, F. P.; Patil, S.; Montenegro, R.; Kietzke, T.; Neher, D.; Scherf, U.; Landfester, K.; List, E. J. W. *Adv. Mater.* **2003,** *15*, 800. Landfester, K.; Montenegro, R.; Scherf, U.; Guntner, R.; Asawapirom, U.; Patil, S.; Neher, D.; Kietzke, T. *Adv. Mater.* **2002**,*14*, 651.

19) Jenekhe, S. A.; Chen, X. L. *Science* **1999**, *283*, 372. Jenekhe, S. A.; Chen, X. L. *Science* **1998**, *279*, 1903.

20) Müller, M.; Zentel, R.; Maka, T.; Romanov, S. G.; Torres, C. M. S. *Adv. Mater.* **2000**, *12*, 1499. Müller, M.; Zentel, R.; Maka, T.; Romanov, S. G.; Torres, C. M. S. *Chem. Mater.* **2000**, *12*, 2508.

21) Holland, B. T.; Stein, A. *Science* **1998,** *281*, 538.

22) Yan, H. W.; Blanford, C. F.; Holland, B. T.; Parent, M.; Smyrl, W. H.; Stein, A. *Adv. Mater*. **1999**, *11*, 1003.

23) Kulinowski, K. M.; Jiang, P.; Vaswani, H.; Colvin, V. L. *Adv. Mater*. **2000**, *12*, 833.

24) Velev, O. D.; Jede, T. A.; Lobo, R. F.; Lenhoff, A. M. *Nature* **1997**, *389*, 447.

25) Blanco, A.; Chomski, E.; Grabtchak, S.; Ibisate, M.; John, S.; Leonard, S. W.; Lopez, C.; Meseguer, F.; Miguez, H.; Mondia, J. P.; Ozin, G. A.; Toader, O.; van Driel, H. M. *Nature* **2000**, *405*, 437.

26) Imhof, A. Pine, D. J. *Nature* **1997***, 389*, 948.

27) Widawski, G. Rawiso, B. Francois, B. *Nature,* **1994,** *369*, 387.

28) Pitois O. Francois, B. *Colloid. Polym. Sci*. **1999**, *277*, 574.

29) Pitois O. Francois, B. *Eur. Phys. J*. **1999,** *B8*, 225.

30) Monnier A.; Schüth, F.; Huo, Q.; Kumar, D.; Margolese, D.; Maxwell, R. S.; Stucky, G. D.; Krishnamurty, M.; Petroff, P.; Firouzi, A.; Janicke, M.; Chmelka, B. F. *Science* **1993**, *261*, 1299.

31) Beck, J. S.; Vartuli, J. C.; Roth, W. J.; Leonowicz, M. E.; Kresge, C. T.; Schmitt, K. D.; Chu, C. T. W.; Olson, D. H.; Sheppard, E. W.; McCullen, S. B.; Higgins, J. B.; Schlenker, J. L. *J. Am. Chem. Soc.* **1992**, *114*, 10834.

32) Kresge, C. T.; Leonowicz, M. E.; Roth, W. J.; Vartuli, J. C.; Beck, J. S. *Nature* **1992**, *359*, 710.

33) Li, Z.; Zhao, W.; Liu, Y.; Rafailovich, M. H.; Sokolov, J.; Khougaz, K.; Eisenberg, A.; Lennox, R. B.; Krausch, G. *J. Am. Chem. Soc*. **1996,** *118*, 10892.

34) Park, M.; Harrison, C.; Chaikin, P. M.; Register, R. A.; Adamson, D. H. *Science* **1997,** *276*, 1401.

35) Morkved, T. L.; Wiltzius, P.; Jaeger, H. M.; Grier, D. G.; Witten, T. A. *Appl. Phys. Lett*. **1994**, *64*, 422.

36) Davis, S. A.; Burkett, S. L.; Mendelson, N. H.; Mann, S. *Nature* **1997**, *385*, 420.

37) Morgenroth, F.; Kübel, C.; Müllen, K. *J. Mater. Chem.* **1997**, *7*, 1207. Wiesler, U. M.; Weil, T.; Müllen, K. *Top. Curr. Chem.* **2001**, *212*, 1.

38) Li, K.; Stover, H. D. H. *J. Polym. Sci. A* **1993**, *31,* 3257. Li, W. H.; Stover, H. D. H. *J. Polym. Sci. A* **1998**, *36,* 1543.

39) Martin, C. R. *Acc. Chem. Res.* **1995**, *28*, 61. Martin, C. R. *Chem. Mater.* **1996**, *8*, 1739.

40) Wilson, J. N.; Bangcuyo, C. G.; Erdogan, B.; Myrick, M. L.; Bunz, U. H. F. *Macromolecules* **2003**, *36*, 1426.

41) Finnefrock, A. C.; Ulrich, R.; Du Chesne, A.; Honeker, C. C.; Schumacher, K.; Unger, K. K.; Gruner, S. M.; Wiesner, U. *Angew. Chem.* **2001**, *40*, 1207.

42) Baker, J. T. *Phil. Mag*. **1922**, *56*, 752.

43) Aitken, J. *Nature,* **1911,** *86*, 516.

44) Beysens, D.; Steyer, A.; Guenoun, P.; Fritter, D.; Knobler, C. M. *Phase Transitions,* **1991,** *31*, 219.

45) Stenzel, M. H. *Aust. J. Chem.* **2002**, *55*, 239.

46) Synthesis of PPEs see: Kloppenburg, L.; Jones, D.; Bunz, U. H. F. *Macromolecules* **1999**, *32*, 4194. Wilson, J. N.; Waybright, S. M.; McAlpine, K.; Bunz, U. H. F. *Macromolecules* **2002,** *35,* 3799.

47) The poly(3-hexylthiophene) **2** was synthesized according to: Amou, S.; Haba, O.; Shirato, K.; Hayakawa, T.; Ueda, M.; Takeuchi, K.; Asai, M. *J. Polym. Sci. A* **1999**, *37,* 1943.

48) Wang, Y. Q.; Erdogan, B.; Wilson, J. N.; Bunz, U. H. F. *Chem. Commun.* **2003**, 1624.

49) See reference 6.

50) (a) Grell, M.; Bradley, D. D. C.; Inbasekaran, M.; Woo, E. P. *Adv. Mater.* **1999**, *9*, 798. (b) Scherf, U.; List, E. J. W. *Adv. Mater.* **2002**, *14*, 477.

51) The polymers **18** and **19** were obtained from Dow Chemicals.